

Universality of neural dynamics on complex networks

Vaiva Vasiliauskaite^{†*} and Nino Antulov-Fantulin[†]

Computational Social Science, ETH Zürich, 8092 Zürich, Switzerland

(Dated: January 13, 2023)

This paper discusses the capacity of graph neural networks to learn the functional form of ordinary differential equations that govern dynamics on complex networks. We propose necessary elements for such a problem, namely, inductive biases, a neural network architecture and a learning task. Statistical learning theory suggests that generalisation power of neural networks relies on independence and identical distribution (i.i.d.) of training and testing data. Although this assumption together with an appropriate neural architecture and a learning mechanism is sufficient for accurate out-of-sample predictions of dynamics such as, e.g. mass-action kinetics, by studying the out-of-distribution generalisation in the case of diffusion dynamics, we find that the neural network model: (i) has a generalisation capacity that depends on the first moment of the initial value data distribution; (ii) learns the non-dissipative nature of dynamics implicitly; and (iii) the model's accuracy resolution limit is of order $\mathcal{O}(1/\sqrt{n})$ for a system of size n .

Introduction Dynamics in a complex networked system is modelled as a set of n ordinary differential equations (ODEs) that describe the rate of change of a quantity $x_i(t)$ for each node i and are coupled via adjacency matrix $\mathbf{A} \in \mathbb{R}^{n \times n}$. A general form of these equations is

$$\begin{aligned} \dot{x}_i &= L(x_i(t)) + \bigoplus_j A_{ij} Q(x_i(t), x_j(t)) \\ &= \mathcal{F}(x_i(t), \mathbf{x}(t), \mathbf{A}) \end{aligned} \quad (1)$$

where L describes self-interactions, Q is a function that models pairwise interactions between neighbours and \bigoplus is an aggregation function. With appropriate choices of functions L , Q , \bigoplus this definition is a general form for models of epidemic processes, biochemical dynamics, birth–death processes, gene regulatory dynamics [1], as well as dynamics that show chaotic behaviour [2].

The initial value problem of a set of ODEs such as Eq. 1 together with an initial condition $\mathbf{x}(t_0)$, has a solution that satisfies

$$\mathbf{x}(t) = \mathbf{x}(t_0) + \int_{t_0}^t \mathcal{F}(\mathbf{x}(t'), \mathbf{A}) dt' \quad (2)$$

and describes a set of trajectories of the dynamics, if the system was initialised at $\mathbf{x}(t_0)$.

Appropriately setup, a neural network $\Psi(\mathbf{x}; \boldsymbol{\omega})$ has capacity to approximate any continuous function F with compact support [3]. In practice, learning the weights is usually done via some variant of backpropagation algorithm [4].

Notably, neural networks can also be used to approximate dynamical systems [5] and find solutions of initial and boundary value problems of differential equations [6]. A dynamical system is that in which \mathcal{F} describes the time dependence of \mathbf{x} in an ambient space. Notably, *if \mathcal{F} is known*, the description quality of the course of dynamics

is independent of a coordinate in the space. For example, Newton's laws of motion describe the trajectory of a bouncing ball regardless of its longitudinal and latitudinal position. Recovering *universal* dynamical principles from empirical data has been shown to belong to NP-hard class [7].

Despite, the hardness of problem, in recent years, different classes of neural networks were used to learn different parts of dynamics from empirical data, including graph neural networks [8] and their differential [9] counterparts [10]; reservoir computers [11, 12] as well as regression techniques [13, 14] or to learn control dynamics [15].

Here we discuss architectural design choices and inductive biases that are crucial for a neural network model that approximates dynamics evolving on complex networks. We then study the model's generalisation capacity using simple models of deterministic dynamics [1]. Lastly, we discuss our work in the context of learning principles that govern dynamics in complex system from perspective of generalization to unseen initial conditions.

Inductive biases for dynamics on complex networks There are several important inductive biases and assumptions worth noting about the complex network dynamics and its neural approximations.

1. Network structure: There exists a known static network represented as an adjacency matrix \mathbf{A} . Therefore it is reasonable to take a GNN [16] as the candidate for Ψ . A single-layer graph convolution network can be defined as

$$\Psi_{gnn}(\mathbf{x}) = (\sigma[\Phi \mathbf{x} \mathbf{W} + \mathbf{b}]) \mathbf{W}_{agg}. \quad (3)$$

where $\mathbf{x} \in \mathbb{R}^{n \times d}$ is an input, $\Phi \in \mathbb{R}^{n \times n}$ is a graph operator (e.g. $\Phi = \tilde{\mathbf{D}}^{-\frac{1}{2}} \tilde{\mathbf{A}} \tilde{\mathbf{D}}^{-\frac{1}{2}}$ [17]), $\mathbf{W} \in \mathbb{R}^{d \times h}$, $\mathbf{b} \in \mathbb{R}^{n \times 1}$, $\mathbf{W}_{agg} \in \mathbb{R}^{h \times d}$ are trainable parameters and σ is a non-linear function. Different versions of GNN with respect to different expressive power for Weisfeiler-Lehman isomorphism are described in [18].

2. Self-Interaction: The model includes a self-interaction part that approximates $L(\cdot)$.

* vvasiliau@ethz.ch

† Authors contributed equally to this work.

3. Neighbour-Interaction: The model includes a neighbour interaction part that approximates $Q(\cdot, \cdot)$. Note that a single-layer GNN, such as a convolutional graph neural network has no mixed quadratic terms $x_i x_j$ and therefore does not simply satisfy such a condition. Although theoretically it should still be possible to approximate nonlinear quadratic terms with a single layer neural network with an arbitrary width, in practice it can be challenging and require either a very large number of hidden neurons, or an exotic learning mechanism that goes beyond the standard gradient descend. Alternatively, one can improve expressivity of the model by increasing its depth, i.e. using multi-layer GNNs or message-passing neural networks [19] to represent $\Psi(\mathbf{x}; \boldsymbol{\omega})$. Here $\boldsymbol{\omega}$ includes graph operator terms $\Phi^k, k \in \{1, 2, \dots, K\}$ where K is the depth of the neural network.

4. Spatiotemporal locality: The dynamical process that follows Eq. 1 must be local, that is, the function $Q(\cdot, \cdot)$ encodes interactions between neighbours. However, including terms Φ^k in a multi-layer graph neural network allows for k -hop interactions via length k walks in a network at a timescale smaller than the infinitesimal dt thereby subdividing dt to k intervals and breaking an assumption of temporal locality.

5. Aggregation of neighbour-interactions: The aggregation can itself be non-linear.

6. Initial value condition: Initial values are preserved during training: $\mathbf{x}_0: \Psi(\mathbf{x}_0) \rightarrow \mathbf{x}_0$. If the neural network straightforwardly approximates the RHS of Eq. 2, then encoding and decoding layers must be pseudo-inverses of each other, see App. A.

7. Conservation/dissipation laws. If the system is closed, it does not exchange energy or mass with the environment, therefore a conservation law holds, namely

$$\sum_i \frac{dx_i(t)}{dt} = C \quad \forall t. \quad (4)$$

A constraint on a neural network to satisfy conservation laws can be imposed via a regularisation term in the loss function,

$$R(\mathcal{D}) = \frac{1}{|\mathcal{D}|} \sum_{\mathbf{x} \in \mathcal{D}} |\mathcal{F}(\mathbf{x})\mathbb{1} - \Psi(\mathbf{x})\mathbb{1}|,$$

that penalises the model weights which produce predictions which do not respect the conservation law Eq. 4. Here \mathcal{D} is the dataset over which the loss is calculated. The strength of the regulariser term can be modulated by multiplying $R(\mathcal{D})$ with a non-negative real number λ .

Architecture Given the inductive biases for dynamics on networks, we propose a neural network model of the following form:

$$\dot{\mathbf{x}} = \boldsymbol{\psi}^\ell(\mathbf{x}) + \boldsymbol{\psi}^\oplus(\mathbf{x}) \quad (5)$$

$$\boldsymbol{\psi}^\oplus(\mathbf{x}) = \text{vec}^{-1} \left(\boldsymbol{\psi}^{q_3} \left\{ \text{vec} \left(\Phi \odot \left(\boldsymbol{\psi}^{q_1}(\mathbf{x})^{\top_1} \times_k \boldsymbol{\psi}^{q_2}(\mathbf{x})^{\top_2} \right) \right) \right\} \right)$$

where $\boldsymbol{\psi}(\mathbf{x})$ is a single hidden layer neural network are given by (3). The mappings of local interaction are summarised in App. B. The design choices of Eq. 5 comply with the inductive biases stated earlier. To this end, we performed vectorisation of input to the function $\boldsymbol{\psi}^\oplus[\boldsymbol{\psi}^{q_3}(\cdot)]$. This function can approximate any invariant poolings of a set [20] or a multiset [18]. Notably, we also assumed that $Q(\cdot, \cdot)$ is factorisable. Since it can be approximated by Chebyshev polynomials, and, according to the strictly real fundamental theorem of algebra [21], it is possible to factorise polynomial function to two factors. Alternatively, one can use deep sets [20] as arguments to approximate $Q(\cdot, \cdot)$.

In order to guarantee the local existence and uniqueness of the solution to the initial value problem, by Picard–Lindelöf theorem the neural network Ψ needs to be Lipschitz continuous. To enforce Lipschitz continuity of Ψ , we will be using 1-Lipschitz activation functions such as ReLU, sigmoid, softmax, or tanh.

Learning task We formulate two distinct statistical learning settings that relate to an increasing strength of generality in the approximation of a dynamical system.

1. Regression task to approximate \mathcal{F} by Ψ : An appropriate “proto data set” here is

$$\mathcal{D} = \{(\mathbf{x}(t)^\alpha, \mathbf{y}(t)^\alpha)\},$$

s.t. $\mathbf{x}(t)^\alpha \in \mathbb{R}^n, \mathbf{y}(t)^\alpha \in \mathbb{R}^n, \mathbf{x}(0)^\alpha \sim f_{x(0)}(x), t = [0, T] \in \mathbb{R}$.

our labels are defined as $\mathbf{y}(t)^\alpha = \mathcal{F}(\mathbf{x}(t)^\alpha)$, α denotes α -th initial condition $\mathbf{x}(0)^\alpha$ sampled from a predefined distribution $f_{x(0)}(x)$; all others points $\mathbf{x}(t)^\alpha$ are obtained following Eq. 2. Here the functional mapping that is being learnt is $\hat{\mathcal{F}}: \mathbb{R}^n \rightarrow \mathbb{R}^n$ and is obtained by minimising the loss \mathcal{L} between the true labels \mathbf{y} and the labels $\mathbf{f}(\mathbf{x})$ obtained by the current model:

$$\hat{\mathcal{F}} = \arg \min_{\mathbf{f}: \mathbb{R}^n \rightarrow \mathbb{R}^n} \mathbb{E}_{\mathcal{P}(\mathbf{x}, \mathbf{y})} \mathcal{L}(\mathbf{f}(\mathbf{x}), \mathbf{y}).$$

Here \mathbb{E} is an expectation operator, $\mathcal{P}(\mathbf{x}, \mathbf{y})$ is the data sampling distribution.

At the moment, samples from the “proto data set” are not independent: those trajectories that were obtained from the same initial condition are non-i.i.d. Such sampling is compulsory for the Uniform Law of Large numbers, that together with capacity control ensures generalisation from train to test set [22, 23]. To ensure statistical independence of samples, we create finite train and test sets of size m_1, m_2 by using a specific distribution P over a “proto data set”

$$\mathcal{D}_{\text{train}} \cup \mathcal{D}_{\text{test}} \sim \mathcal{P}(\mathbf{x}, \mathbf{y}).$$

Specifically, we randomly delegate $(\mathbf{x}(t)^\alpha, \mathbf{y}(t)^\alpha)$ to either $\mathcal{D}_{\text{train}}$ or $\mathcal{D}_{\text{test}}$ thereby ensuring an i.i.d. condition by dropping information on the initial conditions and time.

| Dynamics | L | Q | $\mathcal{L}_{\text{reg}}^{\text{train}}$ | $\mathcal{L}_{\text{reg}}^{\text{test}}$ | \approx_{reg} | $\mathcal{L}_{\text{traj}}^{\text{train}}$ | $\mathcal{L}_{\text{traj}}^{\text{test}}$ | \approx_{traj} |
|-------------------|--------------|---------------------------|---|--|------------------------|--|---|-------------------------|
| Heat ^a | – | $B(x_j - x_i)$ | 2.03 ± 1.03 | 2.14 ± 1.08 | ✓ | 1.39 ± 0.59 | 1.47 ± 0.63 | ✓ |
| MAK ^b | $F - Bx_i^b$ | Rx_j | 0.41 ± 1.08 | 0.44 ± 1.14 | ✓ | 1.48 ± 0.05 | 1.55 ± 0.04 | × |
| PD ^c | $-Bx_i^b$ | Rx_j^a | 4.68 ± 12.82 | 4.72 ± 12.89 | ✓ | 3.03 ± 0.03 | 3.04 ± 0.03 | ✓ |
| MM ^d | $-Bx_i$ | $R \frac{x_j^h}{1+x_j^h}$ | 7.68 ± 5.36 | 7.83 ± 5.47 | ✓ | 5.93 ± 0.12 | 5.94 ± 0.14 | ✓ |
| SIS ^e | $-Bx_i$ | $(1 - x_i)x_j$ | 1.16 ± 3.62 | 1.31 ± 4.07 | ✓ | 1.54 ± 0.01 | 1.64 ± 0.02 | × |

^a $B = 0.05$. ^b $B = 0.1, R = 1, f = 0.5$. ^c $B = 2, R = 0.3, a = 1.5, b = 3$.
^d $B = 4, R = 0.5, h = 3$. ^e $B = 5, R = 0.5$.

TABLE I. Generalisation of a neural network model Eq. 5 trained on dynamics from [1] in the regression task setting, and the trajectory learning setting. Reported loss values are multiplied by a factor 10^{-2} . In columns denoted “ \approx ” we indicate for which dynamics the train loss is approximately similar (“ \checkmark ”) or different (“ \times ”) from the test loss.

2. Trajectory learning setting that approximates $\mathbf{x}(t)$: here the train set contains m_1 initial conditions $\mathbf{x}(0)^\alpha$ as inputs, while each label corresponds to trajectories $\mathbf{y}^\alpha = \{\mathbf{x}(t)^\alpha\}$, where $t = 0, \Delta t, 2\Delta t, \dots, k\Delta t = T$ that were realised from the initial condition $\mathbf{x}(0)^\alpha$:

$$\begin{aligned} \mathcal{D}_{\text{train}} &= \{(\mathbf{x}(0)^\alpha, \mathbf{y}^\alpha)\}, \\ \text{s.t. } \mathbf{x}(0)^\alpha &\in \mathbb{R}^n, \mathbf{y}^\alpha \in \mathbb{R}^{kn}, \mathbf{x}(0)^\alpha \sim f_{x(0)}(x), \alpha \in [1, m_1], \\ \mathbf{y}^\alpha &= \{\mathbf{x}(0)^\alpha, \mathbf{x}(\Delta t)^\alpha, \dots, \mathbf{x}(k\Delta t)^\alpha\} \end{aligned}$$

and test set $\mathcal{D}_{\text{test}}$ is constructed analogously from m_2 initial conditions that are sampled from the same distribution $\mathbf{x}(0)^\alpha \sim f_{x(0)}(x)$. The mapping learnt here is of the following form: $\hat{\mathcal{F}} : \mathbb{R}^n \rightarrow \mathbb{R}^{kn}$ and is realised by computing an initial value problem Eq. 2 using a neural network Ψ in replacement of \mathcal{F} .

Experiments and Results We consider models with $h' = 6, h = 8, h'' = 5, h_d = 3$, trained in 1000 epochs using Adam optimiser with learning rate of 10^{-2} and weight decay 10^{-3} . All activations are ReLU. Unless otherwise stated, the initial values in both the train set and the test set are sampled from $\mathcal{B}[a = 5, b = 5]$. For numerical integration, an explicit Runge-Kutta method of order 5(4) is used [24].

The training loss function is the average L_1 norm. For the regression task, the loss is

$$\mathcal{L}_{\text{reg}}^{\text{train}} = \frac{1}{N_{\text{reg}}} \sum_{\mathbf{x}, \mathbf{y} \in \mathcal{D}_{\text{train}}} \left(\|\mathbf{f}(\mathbf{x}) - \mathbf{y}\|_1 + \lambda R(\mathbf{x}) \right),$$

where $N_{\text{reg}} = |\mathcal{D}_{\text{train}}|(x_{\text{max}} - x_{\text{min}})$. For the trajectory learning task, the loss is defined as:

$$\begin{aligned} \mathcal{L}_{\text{traj}}^{\text{train}} &= \frac{1}{N_{\text{traj}}} \sum_{\mathbf{x}(0), \mathbf{y} \in \mathcal{D}_{\text{train}}} \sum_{k=0}^{T/\Delta t} \\ &\left(\|\mathbf{x}(k\Delta t) - \hat{\mathbf{x}}(k\Delta t)\|_1 + \lambda R(\mathbf{x}(k\Delta t)) \right) \end{aligned} \quad (6)$$

Here the normalisation constant is $N_{\text{traj}} = |\mathcal{D}_{\text{train}}|nT(x_{\text{max}} - x_{\text{min}})/\Delta t$. $\lambda = 0$ and the regularisation terms are nil for the first part of the analysis.

The training sets include samples from 10^3 trajectories, the testing sets – from 10^2 trajectories and the batch size is 10. The parameters for numerical integration are $\Delta t = 0.01, T = 1.5$. In all cases, a graph was sampled from Erdős-Rényi ensemble with $p = 0.5$ and $\oplus = \sum_j$.

Tab. I shows that the trained neural network model Eq. 5 can well-approximate the true dynamics and generalise to unseen initial values well, *provided* $f_{x(0)}(x)$ is used for generating both, a training test and a sampling test.

Generalisation Crucially, the universality of the neural approximation exemplified in Tab. I is only at the *lowest level* that is attainable by putting strong constraints on a test set (that are in accordance with statistical learning theory): the two sets must be statistically equivalent. If the distribution of initial values is irrelevant for the steady state solution, the neural model also inadvertently universally approximates the dynamical system.

However, it seems reasonable to ask if a neural network can do better. In Tab. II we propose three tiers of universality of approximation $\mathcal{F} \approx \Psi$ in terms of statistical properties of training and testing samples. In this context, the statistical learning theory concerns only the lowest level of generality.

| Level | Relation between f and g |
|--------|--|
| Bottom | $f_{X_0} \equiv g_{X_0}$ or $f_{X_0, X_\infty} = f_{X_0} f_{X_\infty}$ |
| Mid | $f_{X_0} \neq g_{X_0}, \sup f_{X_0} = \sup g_{X_0}$ |
| Top | $f_{X_0} \neq g_{X_0}, \sup f_{X_0} \neq \sup g_{X_0}$ |

TABLE II. Generalisation levels for a neural approximation $\mathcal{F} \approx \Psi$ is encompassed in model’s ability to extrapolate predictions to data that was not used during training. Probability density functions related to training data are denoted by “ f ”; related to testing data are denoted by “ g ”.

More sophisticated, *mid* and *top* level generalisations would enable a faithful prediction in cases where the constraints on statistical properties of data are relaxed, for example, where f_{X_0} is not the same as g_{X_0} .

Diffusion A dynamical system whose faith and the course of action depend on the distribution of initial values enables us to study the limits of generalisation of a

neural network. Diffusion equation on a graph is a good example due to its simplicity and known analytical solution of the form

$$\mathbf{x}(t) = \sum_i a_i(0) e^{-B\lambda_i t} \mathbf{v}_i, \quad a_i(0) = \mathbf{x}(0)^\top \mathbf{v}_i, \quad (7)$$

where λ_i, \mathbf{v}_i are i^{th} eigenvalue and eigenvector of the graph Laplacian and the steady state solution is given by

$$\lim_{t \rightarrow \infty} x_i(t) = \frac{1}{n} \sum_j x_j(0) \quad \forall i.$$

Perturbation of the initial value $\mathbf{x}(0)$ by $\delta \sim f_\delta$ such that $x_i^\delta(0) = x_i(0) + \delta$ gives a difference in the steady state solutions of $\langle x_i^\delta(0) \rangle_i - \langle x_i(0) \rangle_i = \gamma$.

Fig. 1 shows how the loss accumulates over the integration time t for the neural network model Ψ for trajectories in the train and in the test sets. In addition, we consider a perturbation (NN,PERT) where the initial value is sampled from a *different* distribution, namely, $g_{X_0}(x) = \mathcal{B}(6, 5)$, while the neural network was trained using $f_{X_0}(x) = \mathcal{B}(5, 5)$. This figure shows that the neural network prediction is reasonable, under i.i.d. sampling condition for an initial condition in train and test set.

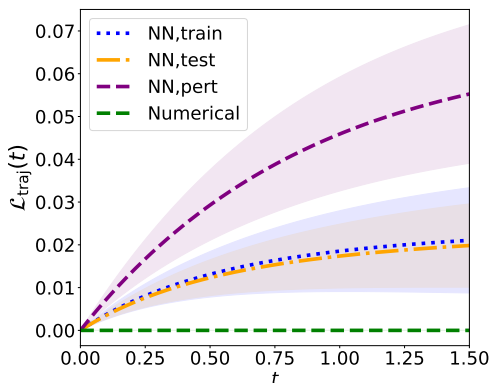


FIG. 1. Node average loss between the analytical solution and: 1) the numerical solution (NUMERICAL), 2) the neural network solution for a subset of initial conditions in the training set (NN,TRAIN) as well as a subset of a testing set (NN,TEST). The original $\mathbf{x}(0) \sim \mathcal{B}(5, 5)$, whereas the perturbed (NN,PERT) initial values $\mathbf{x}'(0) \sim \mathcal{B}(6, 5)$. The loss is computed for the trajectory learning task using $N_{\text{traj}} = 100$ trajectories in each case using an equation $\mathcal{L}_{\text{traj}}(t) = \frac{1}{N_{\text{traj}}} \sum_{\mathbf{x}(0), \mathbf{y} \in \mathcal{D}} \|\mathbf{x}(t) - \hat{\mathbf{x}}(t)\|_1$. The errors show one standard deviation.

Fig. 2 follows the same analysis and shows that by varying the parameters of the beta distribution $\mathcal{B}(a, b)$, the loss in the steady state (averaged over the last 10 steps of the simulation) is proportional to the difference in expectation value of the beta-distribution used in training, and in testing to generate the initial values. All in all, these results show that *the neural network approximation of the differential form is exclusive to the statistical properties of the training set*.

Upsofar, conservation law (4) and the effect of the regulariser were not considered. We study it in Fig. 3 for a small case with a graph composed of $N = 2$ nodes. This figure presents two key findings: Fig. 3a) clearly shows that Ψ is biased towards the training set; whereas in Fig. 3b) it is clear that Ψ has the property of implicit dissipative (conservation) regularization. Even in the case of no explicit regularization of the dissipative term, the neural network optimises towards a less dissipative regime. This is of particular importance, since some systems in Tab. I are non-dissipative and some are dissipative.

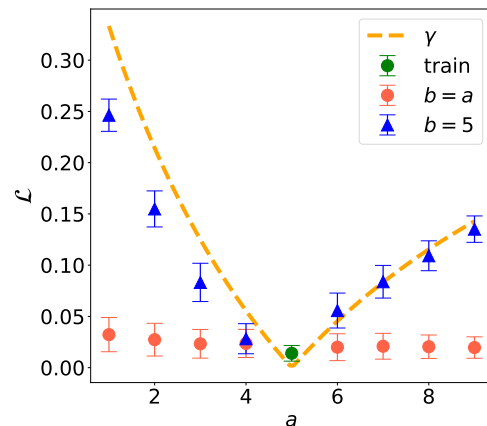


FIG. 2. Generalisation of Ψ to unseen initial conditions. The neural network was trained using initial values sampled from $\mathbf{x}_0 \sim \mathcal{B}(5, 5)$ until it achieved the loss TRAIN. Its prediction capacity was then tested on dynamics with initial conditions $\mathbf{x}_0 \sim \mathcal{B}(a, b = a)$ (red circles) as well as $\mathbf{x}_0 \sim \mathcal{B}(a, b = 5)$ (blue triangles). The dashed orange line is a function $|0.5 - a|/(a + 5)$. The loss is computed for the trajectory learning task using $N_{\text{traj}} = 100$ trajectories in each case using (6), omitting the term $x_{\text{max}} - x_{\text{min}}$ in the normalisation and considering the last 10 timesteps. The errors show one standard deviation across trajectories.

Next, we turn our attention to analyse the out-of-sample loss for system of n coupled differential equations (coupling with Erdős-Rényi model) and diffusion dynamics. Notably, the steady state solution is governed by the average value $\langle \mathbf{x}_0 \rangle$, and since we have n nodes in our system this value has variance $\propto 1/\sqrt{n}$. This implies that *it is easier to accurately predict dynamics with a larger number of differential equations*. In Fig. 4, we show that indeed, test loss is inversely proportional to the system's size.

Discussion In this paper, we proposed a variant of a Neural ODE model which implements a set of inductive biases suitable for complex dynamics on graphs and elicits dynamical models in complex networked systems directly from time series these systems produce. While we showed the presence of generalisation out-of-sample for a wide range of dynamical models, perhaps more importantly such an exercise reflects on generalisation capacity only at the most trivial level. Multiple out-of-distribution

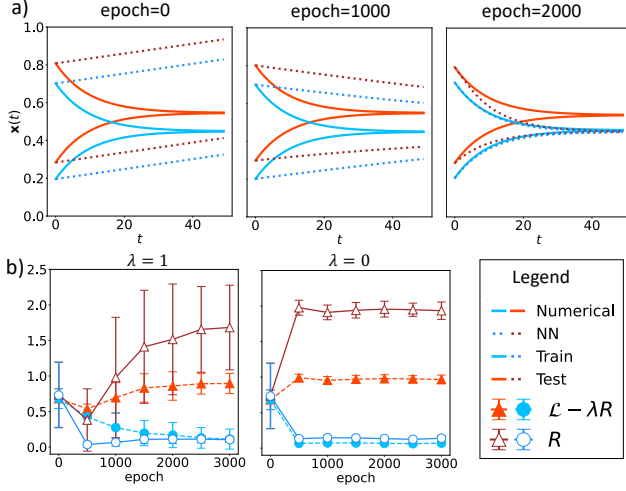


FIG. 3. Learning diffusion on a fully connected $n = 2$ network using the regression training paradigm and a conservation law regulariser. The training sample consists of datapoints obtained from trajectories generated using $\mathbf{x}_0 \sim [0.2, 0.7] + \mathcal{N}(0, 0.1)$, the testing sample: $\mathbf{x}_0 \sim [0.3, 0.8] + \mathcal{N}(0, 0.1)$. **a)** shows an example of a training process, namely by contrasting the true (continuous lines) and learnt (dotted) trajectories of an initial value problem as predicted after indicated training epochs, using $\lambda = 1$. **b)** shows the loss and the value of the regulariser over training period in the case where the regulariser plays a part in training ($\lambda = 1$, same training as in **a)**), and when it does not ($\lambda = 0$). The results in **b)** are obtained from 10 independent runs.

tests suggest that the neural network approximation is valid only for a specific probability distribution of initial values, which was also used to generate the training samples. Furthermore, even if we kept the statistics intact, we observe that it is harder to achieve accurate predictions in small-size systems as opposed to large-scale ones, due to presence of fluctuations that scale as $\mathcal{O}(1/\sqrt{n})$ for a system of size n .

Appendix A: Encoding and decoding layers

Preceding the differential model layer Ψ , one can encode the input via $\Psi^e : \mathbf{x} \in \mathbb{R}^{n \times d} \rightarrow \mathbf{x} \in \mathbb{R}^{n \times d_e}$ [10], in which case, the state space is of $n \times d_e$ dimensions instead of $n \times d$. To revert back to the original $n \times d$ space, a decoding function Ψ^d is used at the end. The embedding respects the initial values iff $\Psi^e = (\Psi^d)^{-1}$. If the encoding and decoding are obtained via linear layers without bias terms, they are represented by matrices $\mathbf{W}_e \in \mathbb{R}^{d \times d_e}$ and $\mathbf{W}_d \in \mathbb{R}^{d_e \times d}$. So after a forward pass, the initial values are modified if $\mathbf{W}_e \mathbf{W}_d \neq \mathbf{I}$. This only holds if the two matrices are inverses to each other. Since these matrices are not square, one can use a Moore-Penrose inverse, which is a generalisation of the traditional inverse. We want \mathbf{W}_d to be a *right* inverse of \mathbf{W}_e ,

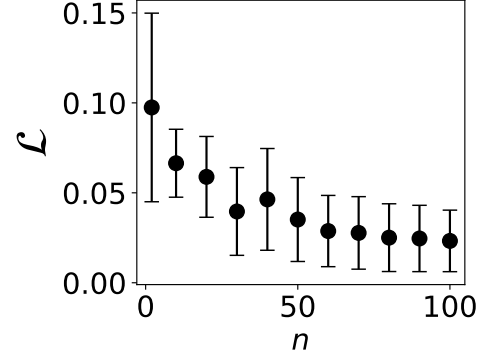


FIG. 4. Test loss (computed for the last 10 time steps of the simulation) for a regression learning task at varied network sizes. The training and testing datasets are sampled from $\mathcal{B}(1, 1)$. Averages are evaluated using 1000 test samples; for training, 100 trajectories were used. The figure indicates that the larger the network, the smaller the average loss and the variance.

defined as: $\mathbf{W}_d = \mathbf{W}_e^* (\mathbf{W}_e \mathbf{W}_e^*)^{-1}$. Here \mathbf{W}_e^* denotes a Hermitian transpose of \mathbf{W}_e , however in our case it is equivalent to a transpose, since \mathbf{W}_e is defined over real numbers.

Appendix B: Neural network mappings

The mappings of functions that constitute the neural network model defined in Eq. 3 are defined as (here we consider input $\mathbf{x} \in \mathbb{R}^{n \times 1 \times d}$, a three-dimensional tensor, and tensor dimension is counted starting from 1):

1. $\psi^\ell : \mathbb{R}^{n \times 1 \times d} \rightarrow \mathbb{R}^{n \times 1 \times d}$, $k = 3$ mode product with $\mathbf{W} \in \mathbb{R}^{d \times h'}$ i.e. $\mathbb{R}^{n \times 1 \times d} \times_3 \mathbb{R}^{d \times h'} \in \mathbb{R}^{n \times 1 \times h'}$ and $\mathbf{C} \in \mathbb{R}^{h' \times d}$.
2. $\psi^{q1}, \psi^{q2} : \mathbb{R}^{n \times 1 \times d} \rightarrow \mathbb{R}^{n \times 1 \times h}$, $k = 3$ mode product with $\mathbf{W} \in \mathbb{R}^{d \times h}$: $\mathbb{R}^{n \times 1 \times d} \times_3 \mathbb{R}^{d \times h} \in \mathbb{R}^{n \times 1 \times h}$ and $\mathbf{C} = \mathbf{I}$.
3. $\mathbf{x}^{\top 1} : \mathbb{R}^{n \times 1 \times h} \rightarrow \mathbb{R}^{h \times n \times 1}$.
4. $\mathbf{x}^{\top 2} : \mathbb{R}^{n \times 1 \times h} \rightarrow \mathbb{R}^{h \times 1 \times n}$.
5. $(\psi^{q1}(\mathbf{x})^{\top 1} \times_k \psi^{q2}(\mathbf{x})^{\top 2}) : \mathbb{R}^{h \times n \times 1} \times_3 \mathbb{R}^{h \times 1 \times n} \in \mathbb{R}^{h \times n \times n}$.
6. $\Phi \odot (\psi^{q1}(\mathbf{x})^{\top 1} \times_k \psi^{q2}(\mathbf{x})^{\top 2}) : \mathbb{R}^{n \times n} \odot \mathbb{R}^{h \times n \times 1} \times_3 \mathbb{R}^{h \times 1 \times n} \in \mathbb{R}^{h \times n \times n}$. Here an operator \odot denotes a standard “broadcasted” element-wise multiplication.
7. $\text{vec}(\cdot) : \mathbb{R}^{h \times n \times n} \rightarrow \mathbb{R}^{n^2 h \times 1}$.
8. $\psi^{q3} : \mathbb{R}^{n^2 h \times 1} \rightarrow \mathbb{R}^{n^2 h \times 1}$, $\mathbf{W} \in \mathbb{R}^{1 \times h''}$ and $\mathbf{C} \in \mathbb{R}^{h'' \times 1}$.
9. $\text{vec}^{-1}(\cdot) : \mathbb{R}^{n^2 h \times 1} \rightarrow \mathbb{R}^{n \times n \times h}$.

10. $\psi^\oplus = \psi(\bigoplus(\cdot))$, where we use $\bigoplus(\cdot)$ as invariant pooling layer $\mathbb{R}^{n \times nh} \rightarrow \mathbb{R}^{n \times 1}$ and then apply de-

coding layer ψ that maps $\mathbb{R}^{n \times 1} \rightarrow \mathbb{R}^{n \times d}$, with $\mathbf{W} \in \mathbb{R}^{1 \times h_d}$ and $\mathbf{C} \in \mathbb{R}^{h_d \times d}$.

-
- [1] B. Barzel and A. L. Barabási, Universality in network dynamics, *Nature Physics* 2013 9:10 **9**, 673 (2013).
- [2] J. C. Sprot, Chaotic dynamics on large networks, *Chaos: An Interdisciplinary Journal of Nonlinear Science* **18**, 023135 (2008).
- [3] K. Hornik, M. Stinchcombe, and H. White, Multilayer feedforward networks are universal approximators, *Neural networks* **2**, 359 (1989).
- [4] D. E. Rumelhart, G. E. Hinton, and R. J. Williams, Learning representations by back-propagating errors, *nature* **323**, 533 (1986).
- [5] K. i. Funahashi and Y. Nakamura, Approximation of dynamical systems by continuous time recurrent neural networks, *Neural Networks* **6**, 801 (1993).
- [6] I. E. Lagaris, A. Likas, and D. I. Fotiadis, Artificial neural networks for solving ordinary and partial differential equations, *IEEE Transactions on Neural Networks* **9**, 987 (1998).
- [7] T. S. Cubitt, J. Eisert, and M. M. Wolf, Extracting dynamical equations from experimental data is np hard, *Phys. Rev. Lett.* **108**, 120503 (2012).
- [8] C. Murphy, E. Laurence, and A. Allard, Deep learning of contagion dynamics on complex networks, *Nature Communications* **12**, 10.1038/s41467-021-24732-2 (2021).
- [9] R. T. Chen, B. Amos, and M. Nickel, Learning neural event functions for ordinary differential equations, *arXiv preprint arXiv:2011.03902* (2020).
- [10] C. Zang and F. Wang, Neural Dynamics on Complex Networks, in *Proceedings of the ACM SIGKDD International Conference on Knowledge Discovery and Data Mining* (Association for Computing Machinery, 2020) pp. 892–902.
- [11] K. Srinivasan, N. Coble, J. Hamlin, T. Antonsen, E. Ott, and M. Girvan, Parallel Machine Learning for Forecasting the Dynamics of Complex Networks, *Physical Review Letters* **128**, 10.1103/PhysRevLett.128.164101 (2022).
- [12] J. Pathak, B. Hunt, M. Girvan, Z. Lu, and E. Ott, Model-free prediction of large spatiotemporally chaotic systems from data: A reservoir computing approach, *Physical review letters* **120**, 024102 (2018).
- [13] T.-T. Gao and G. Yan, Autonomous inference of complex network dynamics from incomplete and noisy data 10.1038/s43588-022-00217-0.
- [14] S. Maddu, B. L. Cheeseman, C. L. Müller, and I. F. Sbalzarini, Learning physically consistent differential equation models from data using group sparsity, *Physical Review E* **103**, 042310 (2021).
- [15] L. Böttcher, N. Antulov-Fantulin, and T. Asikis, Ai ponytryagin or how artificial neural networks learn to control dynamical systems, *Nature communications* **13**, 1 (2022).
- [16] F. Scarselli, M. Gori, A. C. Tsoi, M. Hagenbuchner, and G. Monfardini, The graph neural network model, *IEEE Transactions on Neural Networks* **20**, 61 (2009).
- [17] T. N. Kipf and M. Welling, Semi-Supervised Classification with Graph Convolutional Networks, .
- [18] K. Xu, W. Hu, J. Leskovec, and S. Jegelka, How powerful are graph neural networks?, *arXiv preprint arXiv:1810.00826* (2018).
- [19] K. Xu, S. Jegelka, W. Hu, and J. Leskovec, How Powerful are Graph Neural Networks?, 7th International Conference on Learning Representations, ICLR 2019 10.48550/arxiv.1810.00826 (2018).
- [20] M. Zaheer, S. Kottur, S. Ravanbakhsh, B. Póczos, R. R. Salakhutdinov, and A. J. Smola, Deep sets, *Advances in neural information processing systems* **30** (2017).
- [21] S. Basu, Strictly real fundamental theorem of algebra using polynomial interlacing, *Bulletin of the Australian Mathematical Society* **104**, 249 (2021).
- [22] T. Hastie, R. Tibshirani, J. H. Friedman, and J. H. Friedman, *The elements of statistical learning: data mining, inference, and prediction*, Vol. 2 (Springer, 2009).
- [23] C. Cortes, V. Vapnik, and L. Saitta, *Machine Learning*, Tech. Rep. (1995).
- [24] L. F. Shampine, Some practical runge-kutta formulas, *Mathematics of Computation* **46**, 135 (1986).